Static, oscillating modulus, and moving pulses in the one-dimensional quintic complex Ginzburg-Landau equation: An analytical approach

Orazio Descalzi
Facultad de Ingeniería, Universidad de los Andes, Av. San Carlos de Apoquindo 2200, Santiago de Chile, Chile
(Received 19 March 2004; revised manuscript received 25 July 2005; published 17 October 2005)

By means of a matching approach we study analytically the appearance of static and oscillating-modulus pulses in the one-dimensional quintic complex Ginzburg-Landau equation without nonlinear gradient terms. When considering nonlinear gradient terms the method enables us to calculate the velocities of the stable and unstable moving pulses. We focus on this equation since it represents a prototype envelope equation associated with the onset of an oscillatory instability near a weakly inverted bifurcation. The results obtained using the analytic approximation scheme are in good agreement with direct numerical simulations. The method is also useful in studying other localized structures like holes.

DOI: 10.1103/PhysRevE.72.046210 PACS number(s): 82.40.Bj, 05.70.Ln, 47.20.Ky

I. INTRODUCTION

In the last decade experimental evidence of localized structures in dissipative systems far from equilibrium has been reported. In a quasi-one-dimensional system, an annulus filled with a mixture of ethanol and water and heated from below, localized structures of convection surrounded by nonconvecting fluid have been studied [1]. More recently, the formation of clusters of localized structures via the self-completion scenario in a quasi-two-dimensional gas discharge system [2], and the interaction of dissipative localized structures in an optical pattern-forming system have been observed [3]. Experiments on vertically vibrated granular layers in evacuated containers reveal a variety of patterns including particlelike localized excitations (oscillons) [4]. In chemical systems, catalytic oxidation of CO on Pt(110) exhibits oscillatory kinetics giving rise to solitary waves [5], and experiments on a ferrocyanide-iodate-sulfite reaction diffusion system show spot patterns that undergo a continuous process of growth through replication and death by overcrowding [6].

The wide range of qualitatively different localized structures cannot be understood with a single mechanism. Coexistence between two stable states (not necessarily homogeneous [7]) or excitability are common features of the dynamics of nonequilibrium media that facilitates the formation of localized patterns.

Reaction-diffusion models have been successfully showing a rich variety of behaviors, such as self-replication [8,9], elastic behavior upon collision [10,11], or soliton behavior [12]. Localized solutions have been observed in monostable and bistable systems with two stable fixed points and one unstable fixed point [13] or one stable fixed point, a stable limit cycle, and an unstable limit cycle [12,14,15].

Localized solutions, like pulses, and their interactions have also been studied within the framework of envelope equations and order parameters equations [16,17]. In the domain of the envelope equations, the quintic complex Ginzburg-Landau equation (CGLE) is known to admit stable localized solutions like pulses as a consequence of the coexistence between a stable limit cycle and a stable fixed point and its nonvariational nature. The quintic CGLE represents an important prototype equation, since it arises generically as an envelope equation for a weakly inverted bifurcation associated to traveling waves.

Since Thual and Fauve showed [18] that a quintic CGLE with a destabilizing cubic term gives rise to stable localized solutions, much effort has been performed in studying pulse solutions in this equation from a numerical and analytic point of view. Perturbative analysis of solitons in the nonlinear Schroedinger equation limit (conservative limit) has been developed by some authors [19,20]. The opposite limit (variational limit) has been studied in [21,22]. Particular solutions of the quintic CGLE have been found by van Saarloos and Hohenberg reducing this equation to a three-variable dynamical system [23,24]. These authors pointed out the fact (from a numerical observation) that stationary pulses exist in a narrow range where there is coexistence between zero and the homogeneous solution. Exact solitary wave solutions of the one-dimensional quintic CGLE are obtained using a method derived from the Painlevé test for integrability [25]. These solutions are expressed in terms of hyperbolic functions, and include the pulses found by van Saarloos and Hohenberg. In a series of articles Akhmediev *et al.* report numerical observation of new forms of stable localized solutions of the quintic CGLE including moving pulses. Besides this, they find analytic solutions using a restrictive Ansatz [26–30]. In [31] Deissler and Brand find numerically that there are—in addition to the stationary pulses reported previously—stable localized solutions that are periodic, quasiperiodic, or even chaotic in time. The same authors, in a later article, study the effect of nonlinear gradients terms on breathing localized solutions in the quintic CGLE [32]. In a recent analytical short paper, we have reported a method which enables us to construct approximate analytic stationary pulses in the quintic CGLE in a particular case, namely, without dispersive terms, and to show that the appearance of stationary pulses is related to a saddle-node bifurcation [33]. The method consists of calculating the pulse inside and outside the core and then to match the approximate solutions in the border of the regions, imposing there continuity of the amplitude, the phase, and the derivative of the amplitude.

Our analytical study remains valid through the whole intermediate range of parameters between the variational and the conservative limits. This method has been useful in studying localized oscillating solutions in simple reaction-diffusion systems since at leading order this problem can be reduced to a quintic CGLE without dispersive terms [34].

The goal of this paper is to show in detail the above-mentioned analytical method, not restricted to a particular case, as it was shown in [33], but in the full case, namely the quintic CGLE including dispersive and nonlinear gradient terms. The dispersive terms are responsible, as it has been pointed out in [31], for breathing and chaotic pulses. On the other hand, the quintic CGLE with nonlinear gradient terms is a more general model with application in propagation of ultrashort pulses in optical fibers [35]. In addition, we show how this method can be useful in studying other kinds of localized structures, like holes, in the quintic CGLE.

II. THE QUINTIC CGLE WITHOUT NONLINEAR GRADIENT TERMS: STATIC AND OSCILLATING-MODULUS PULSES

The quintic CGLE without regard to nonlinear gradient terms reads

$$\partial_t A = \mu A + \beta|A|^2 A + \gamma|A|^4 A + D\partial_{xx} A. \tag{1}$$

The subscript x denotes partial derivative with respect to x, $A(x,t)=r(x,t)e^{i\phi(x,t)}$ is a complex field, and the parameters $\beta=\beta_r+i\beta_i$, $\gamma=\gamma_r+i\gamma_i$, and $D=D_r+iD_i$ are, in general, complex. The signs of the parameters $\beta_r>0$ and $\gamma_r<0$ are chosen in order to guarantee that the bifurcation is subcritical and saturates to quintic order. The control parameter μ is considered real. Equation (1) admits a class of homogeneous time-periodic solutions

$$A_{1,2} = r_{1,2} e^{i([\beta_i r_{1,2}^2 + \gamma_i r_{1,2}^4]t + \phi_0)}, \tag{2}$$

where $r_{1,2}^2=\beta_r \pm \sqrt{\beta_r^2+4|\gamma_r|\mu}/2|\gamma_r|$ and ϕ_0 is an arbitrary phase. The existence of $A_{1,2}$ requires that $\mu \geqslant -(\beta_r^2/4|\gamma_r|)$. However inside this range only A_1 is stable against small perturbations. It is easy to see that $A_0=0$ is also a solution of Eq. (1) but it is stable only for $\mu<0$. Therefore the stable solutions A_0 and A_1 coexist for $-(\beta_r^2/4|\gamma_r|)\leqslant\mu\leqslant 0$. Inside this coexistence range is where we are looking for localized solutions.

A. Static pulses

We look for localized solutions of Eq. (1) making the Ansatz [18]

$$A = R_0(x)\exp\{i[\Omega t + \theta_0(x)]\}, \tag{3}$$

where Ω is the oscillation frequency of the pulse which is an unknown parameter to be determined. Replacing (3) in (1) and after an algebra we obtain the following equations for $R_0(x)$ and θ_{0x}:

$$0 = \mu_+ R_0 + \beta_+ R_0^3 + \gamma_+ R_0^5 + R_{0xx} - R_0\theta_{0x}^2, \tag{4}$$

$$\mu_- R_0 = \beta_- R_0^3 + \gamma_- R_0^5 + 2R_{0x}\theta_{0x} + R_0\theta_{0xx}, \tag{5}$$

where

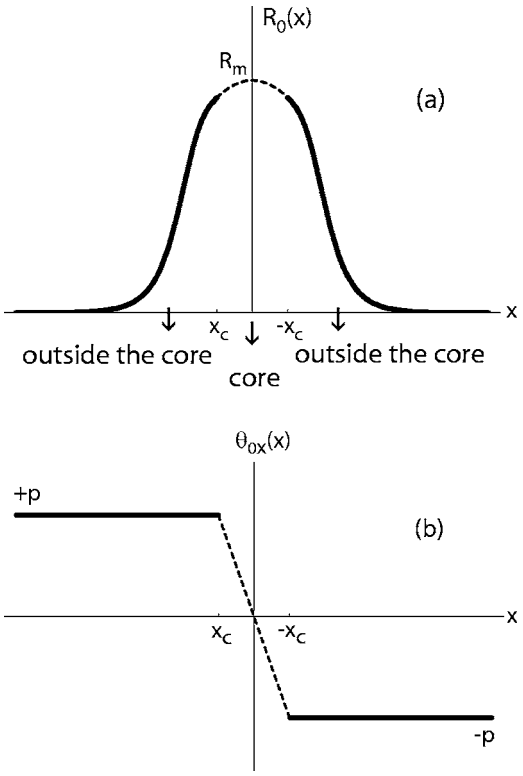

FIG. 1. Analytical approximation for the pulse. The space is divided in two regions: outside the core (drawn as a continuous line), where the wave vector is constant, and core (drawn as a dashed line), where the wave vector is a straight line. (a) Modulus of the pulse. (b) Wave vector.

$$\mu_+ = \frac{D_r\mu - D_i\Omega}{|D|^2}; \quad \beta_+ = \frac{D_r\beta_r + D_i\beta_i}{|D|^2};$$

$$\gamma_+ = \frac{D_r\gamma_r + D_i\gamma_i}{|D|^2}; \quad \mu_- = \frac{D_i\mu + D_r\Omega}{|D|^2};$$

$$\beta_- = \frac{D_r\beta_i - D_i\beta_r}{|D|^2};$$

$$\gamma_- = \frac{D_r\gamma_i - D_i\gamma_r}{|D|^2}, \quad |D|^2 = D_r^2 + D_i^2.$$

In order to solve approximately (4) and (5) we use the following strategy: we consider that θ_{0x} (the wave vector) is constant ($+p$ for the left side and $-p$ for the right side) in almost all the domain (outside the core) except in a narrow domain around the center of the pulse (core), where θ_{0x} is considered to be a straight line [see Fig. 1(b)].

Inside the core we approximate the functions $R_0(x)$ and θ_{0x} by their first terms in a Taylor expansion writing

$$R_0(x) = R_m - \epsilon x^2, \quad \theta_{0x} = -\alpha x, \tag{6}$$

where (R_m, ϵ, α) are unknown quantities. Replacing (6) in (4) and (5) we obtain ϵ and α in terms of (Ω, R_m) and the parameters of (1): $\epsilon=\frac{1}{2}(\mu_+ R_m + \beta_+ R_m^3 + \gamma_+ R_m^5)$, $\alpha=\beta_- R_m^2 + \gamma_- R_m^4 - \mu_-$.

Outside the core where the wave vector θ_{0x} is constant ($+p$ for $x<x_c$ and $-p$ for $x>-x_c$) we can integrate explicitly Eq. (4). The result is

$$R_0(x)=\frac{2b^{1/4}\exp\{\sqrt{-\mu_+ +p^2}(|x|+x_0)\}}{\sqrt{\left[\exp\{2\sqrt{-\mu_+ +p^2}(|x|+x_0)\}+\frac{a}{\sqrt{b}}\right]^2-4}}, \quad (7)$$

where $a=-3\beta_+/2\gamma_+$, $b=-3(-\mu_+ +p^2)/\gamma_+$, and x_0 is a constant to be determined, which is a consequence of the translation symmetry of the CGLE.

Notice that this expression for $R_0(x)$ captures the shape of the pulse in almost all the domain except in the core where the modulus of the pulse has been approximated by a parabola with a maximum R_m. Since Ω is a constant, asymptotically for $|x|\to\infty$ Eqs. (4) and (5) give

$$\Omega=\frac{1}{D_r^2}[-D_i(\mu D_r-2p^2|D|^2)+2p|D|^2\sqrt{-\mu D_r+p^2|D|^2}]. \quad (8)$$

The continuity of $R_0(x)$ at $x=x_c=-p/\alpha$ yields the value of x_0 in terms of R_m and p: $x_0=x_c+(\ln u_c/\sqrt{-\mu_+ +p^2})$, where $u_c^2=-(a/\sqrt{b})+2\sqrt{b}/r_c^2+2/r_c^2\sqrt{r_c^4-ar_c^2+b}$ and $r_c=R_m-\epsilon x_c^2$.

The continuity of the first derivative of $R_0(x)$ at $x=x_c$ gives us the first relation between R_m and p:

$$f(p,R_m)\equiv\sqrt{-\frac{\gamma_+}{3}}r_c\sqrt{r_c^4-ar_c^2+b}+2\epsilon x_c=0. \quad (9)$$

A second relation between R_m and p (a *consistency condition*) is obtained multiplying Eq. (5) by $R_0(x)$ and integrating on the real axis. Since $R_0(x)$ is a symmetric function, the result can be written as

$$g(p,R_m)\equiv\mu_- -\beta_-\frac{\int_{-\infty}^{0}R_0^4\,dx}{\int_{-\infty}^{0}R_0^2\,dx}-\gamma_-\frac{\int_{-\infty}^{0}R_0^6\,dx}{\int_{-\infty}^{0}R_0^2\,dx}=0. \quad (10)$$

The above integrals can be explicitly evaluated. Thus we have constructed approximate expressions for $R_0(x)$ and θ_{0x} in all the domain in terms of two unknown parameters, namely, R_m and p. The existence of static pulses is related to the intersection between the curves $f(p,R_m)=0$ and $g(p,R_m)=0$.

For parameters selected from optical transmission systems [35], we show in Fig. 2 the generic mechanism of appearance and attenuation of the pulses: there exists a critical value μ_c so that for $\mu<\mu_c$ the curves $f(p,R_m)=0$ (continuous line) and $g(p,R_m)=0$ (dashed line) do not intersect at any point suggesting there are no pulses. For $\mu>\mu_c$ the curves intersect in two points giving rise to a stable and an unstable pulse via a saddle-node bifurcation. For these parameters at $\mu=0$ the amplitude of the unstable pulse goes to zero. Thus we conclude that for this set of parameters pairs of stable and unstable pulses exist for $\mu_c<\mu<0$. The authors in Ref. [35]

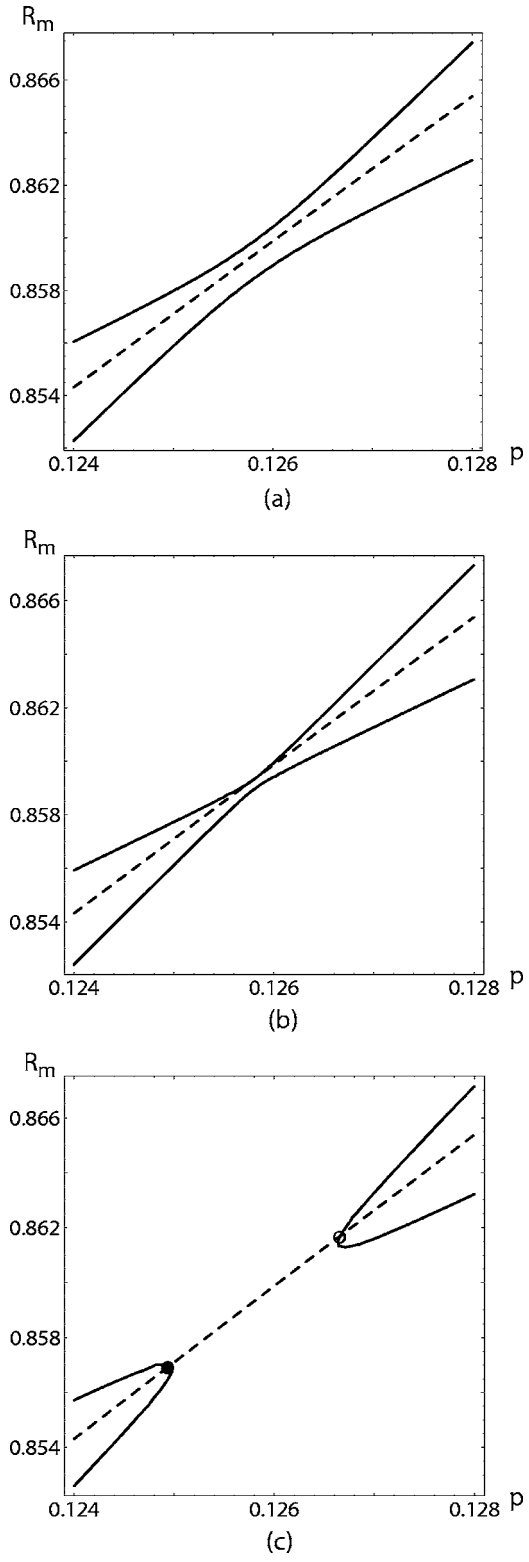

FIG. 2. Saddle-node bifurcation. Values of the parameters are $\beta_r=0.5$; $\beta_i=1$; $\gamma_r=-0.34$; $\gamma_i=0$; $D_r=0.3$; $D_i=0.5$. (a) $\mu=-0.102\,985<\mu_c$. (b) $\mu=\mu_c=-0.102\,983$. (c) $\mu=-0.102\,98>\mu_c$. The intersection between the curves $f(p,R_m)=0$ (continuous line) and $g(p,R_m)=0$ (dashed line) predicts one unstable pulse (solid circle) and one stable pulse (open circle).

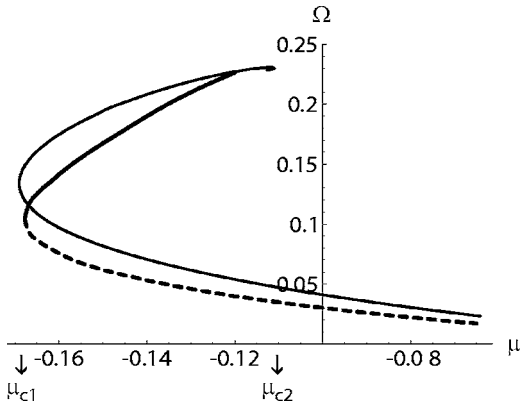

FIG. 3. Bifurcation diagram for pulses. Values of the parameters are $\beta_r=1.0$; $\beta_i=0.2$; $\gamma_r=-1.0$; $\gamma_i=0.15$; $D_r=1.0$; $D_i=-0.1$. The theoretical bifurcation curve is drawn as a thick line (continuous line stands for stable pulses and dashed line stands for unstable pulses). The bifurcation curve computed with software AUTO 2000 is drawn as a thin continuous line.

report a numerical value of μ_c near to -0.09 which is in agreement with our approximate analytical value $\mu_c=-0.102$.

The most general situation is shown in Fig. 3: there exists a critical value μ_{c1} so that for $\mu<\mu_{c1}$ the curves $f(p,R_m)=0$ and $g(p,R_m)=0$ do not intersect at any point. For $\mu>\mu_{c1}$ the curves intersect in two points leading to a stable and an unstable pulse via a saddle-node bifurcation. A saddle-node bifurcation (normally) gives rise to a stable and an unstable solution. In our case it has been confirmed with the software AUTO 2000 [36]. By further increasing μ we find another critical value μ_{c2} so that for $\mu>\mu_{c2}$ there still exists an intersection between the curves $f=g=0$ predicting an unstable pulse, but the stable pulse disappears because there is no intersection between the curves $\mathrm{Re}\, f=\mathrm{Im}\, f=0$ and $\mathrm{Re}\, g=\mathrm{Im}\, g=0$. This second bifurcation is associated with the appearance of fronts.

In Fig. 3 we computed Ω as a function of μ using the expression given by (8) (thick continuous line stands for stable pulses and thick dashed line stands for unstable pulses) and we compare with the curve obtained using the bifurcation software AUTO 2000 [36] (thin continuous line). For values of the parameters $\beta_r=1.0$, $\beta_i=0.2$, $\gamma_r=-1.0$, $\gamma_i=0.15$, $D_r=1.0$, and $D_i=-0.1$ AUTO 2000 shows that near $\mu=-0.168$ and $\mu=-0.11$ the system undergoes a saddle-node bifurcation [see also Refs. [23,24]]. Both critical values of μ are in very good agreement with the theoretical predicted values for $\mu_{c1}=-0.167\,76$ and $\mu_{c2}=-0.1195$. Moreover, both curves show that the branch corresponding to the unstable pulses persists up to $\mu=0$.

To compare the shape of the analytical pulses with those obtained by direct numerical simulations we fix $\mu=-0.13$ and the other parameters as in Fig. 3. Owing to the fact that the curves $f(p,R_m)=0$ and $g(p,R_m)=0$ cut at two points, namely, $p=0.080\,72$; $R_m=0.537\,686$ and $p=0.262\,542$; $R_m=0.909\,28$, we predict two pulses. In Fig. 4(a) we show the shapes of the pulses obtained with our analytical approach. The continuous line corresponds to the stable pulse and the dashed line to the unstable one. The stable pulse obtained

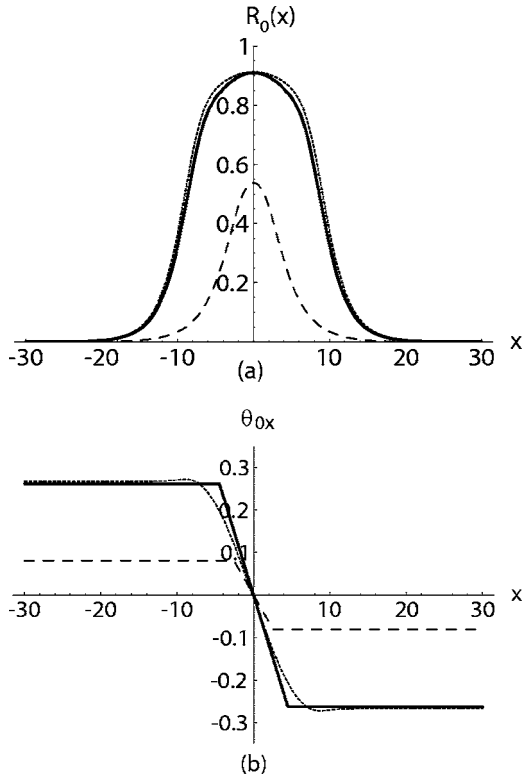

FIG. 4. (a) Shape of the stable and unstable pulses predicted by the analytical approach (continuous and dashed lines). The numerical result for the stable pulse is represented by a punctured line. (b) The wave vector. Values of the parameters are: $\mu=-0.13$; $\beta_r=1.0$; $\beta_i=0.2$; $\gamma_r=-1.0$; $\gamma_i=0.15$; $D_r=1.0$; $D_i=-0.1$.

from the direct numerical simulation is drawn with a punctured line. The values of R_m and the asymptotical value of the wave vector agree within 1% with our analytical approach. In Fig. 4(b) we show the wave vector for the three above-mentioned cases.

The approximation scheme presented here remains valid through the whole intermediate range of parameters between the variational and the conservative limits. We remark by the fact that our approximate solutions are not fully analytic (ultimately, equations for R_m and p have to be numerically solved).

B. Oscillating-modulus pulses

Depending on the parameters, it may happen that before expanding, the fixed-modulus pulse looses its stability against an oscillating-modulus pulse. By further increasing the bifurcation parameter μ this periodic breathing motion becomes quasiperiodic, or chaotic [31].

To study this situation we proceed to consider perturbations of the basic state (fixed-modulus pulse) of the form $r=R_0(x)+\rho(x,t)$; $\phi=\Omega t+\theta_0(x)+\varphi(x,t)$. Substituting these expressions into Eq. (1), linearizing in $\rho(x,t)$ and $\varphi(x,t)$, we obtain

$$\rho_t=(\mu+3\beta_r R_0^2+5\gamma_r R_0^4-D_r\theta_{0x}^2-D_i\theta_{0xx})\rho-2D_i\theta_{0x}\rho_x+D_r\rho_{xx}-2(D_r R_0\theta_{0x}+D_i R_0)\varphi_x-D_i R_0\varphi_{xx},$$

$$R_0\varphi_t = (-\Omega + 3\beta_i R_0^2 + 5\gamma_i R_0^4 + D_r\theta_{0xx} - D_i\theta_{0x}^2)\rho + 2D_r\theta_{0x}\rho_x + D_i\rho_{xx} + 2(D_r R_{0x} - D_i R_0\theta_{0x})\varphi_x + D_r R_0\varphi_{xx}. \quad (11)$$

Asymptotically, i.e, $x\to\infty$; $\theta_{0x}=-p$; $R_0\to 0$ and $R_{0x}/R_0=-\sqrt{-\mu_+ + p^2}$, the system (11) reduces to the following linear system:

$$\rho_t = (\alpha_1 + 2D_i p\partial_x + D_r\partial_x^2)\rho + (\alpha_2 - D_i\partial_x)y,$$

$$y_t = (\beta_1 + \beta_2\partial_x + \beta_3\partial_x^2 + D_i\partial_x^3)\rho + (\beta_4 + 2D_i p\partial_x + D_r\partial_x^2)y, \quad (12)$$

where we have used the following definitions $y\equiv R_0\varphi_x$; $\alpha_1=\mu-D_r p^2$; $\alpha_2=D_i\sqrt{-\mu_+ + p^2}+2D_r p$; $\beta_1=-\sqrt{-\mu_+ + p^2}(\Omega+D_i p^2)$; $\beta_2=-(2D_r p\sqrt{-\mu_+ + p^2}+\Omega+D_i p^2)$; $\beta_3=D_i\sqrt{-\mu_+ + p^2}-2D_r p$; $\beta_4=2D_i p\sqrt{-\mu_+ + p^2}-D_r(-\mu_+ + p^2)$.

Assuming that the functions ρ and y are of the form $\binom{\rho}{y}=\Sigma_k\binom{\rho_k}{y_k}e^{ikx+\sigma_k t}$ system (12) leads to a matrix equation. The condition that a solution exists results in the following equation for σ_k:

$$(\alpha_1 - D_r k^2 + 2iD_i pk - \sigma_k)(\beta_4 + 2iD_i pk - D_r k^2 - \sigma_k) - (\alpha_2 - iD_i k)(\beta_1 + i\beta_2 k - \beta_3 k^2 - iD_i k^3) = 0. \quad (13)$$

Let $\sigma=\mathrm{Re}\,\sigma_k$; then from the above equation we get a relation between σ and the wave number k:

$$b_1 - b_2\sigma + \frac{a_2(a_1 - a_2\sigma)}{(a_3 - 2\sigma)} + \sigma^2 - \frac{(a_1 - a_2\sigma)^2}{(a_3 - 2\sigma)^2} = 0, \quad (14)$$

where $a_1=(2D_i p\alpha_1-\alpha_2\beta_2+D_i\beta_1+2D_i p\beta_4)k+(\alpha_2-4D_r p-\beta_3)D_i k^3$; $a_2=4D_i pk$; $a_3=\alpha_1-2D_r k^2$; $b_1=\alpha_1\beta_4-\alpha_2\beta_1+[\alpha_2\beta_3-D_r(\alpha_1+\beta_4)-D_i\beta_2-4D_i^2 p^2]k^2+|D|^2k^4$; $b_2=\alpha_1-2D_r k^2+\beta_4$.

Thus by increasing the bifurcation parameter μ, for fixed parameters β, γ, and D, it might be possible that above a critical value $\mu=\mu_0$, σ becomes positive for some range of k. Because of the asymptotic linear analysis the existence of μ_0 is an indication that for $\mu>\mu_0$, in the range where one has coexistence of homogeneous attractors, the fixed-modulus pulses are going to loose their stability against oscillating-modulus pulses.

To verify this analytical prediction in a concrete case we fix the parameters of (1): $\beta_r=1.0$, $\beta_i=0.2$, $\gamma_r=-1.0$, $\gamma_i=0.15$, $D_r=1.0$ and $D_i=-0.1$. According to [23,24] there is a range of the bifurcation parameter μ where there exist only stationary pulses with fixed shape. The lower and upper limits of this region have been studied in the previous section (see Fig. 3). Now we proceed to examine $\sigma(k)$ inside this range. The result is that $\sigma(k)$ is negative for all wave number k in the range $\mu_{c1}<\mu<\mu_{c2}$. Therefore our prediction is that there are no oscillating-modulus pulses, which is consistent with numerical observations. Now we choose a different set of parameters: $\beta_r=3.0$, $\beta_i=1.0$, $\gamma_r=-2.75$, $\gamma_i=1.0$, $D_r=0.9$, and $D_i=-1.1$. Plotting $\sigma(k)$ we see in Fig. 5 that it vanishes at $k=0.535$ predicting that the basic state will loose stability for $\mu>\mu_0=-0.295$. For $\mu<\mu_0$ the function $\sigma(k)$ is negative for all k. Numerical simulations of Eq. (1) show that for these parameters the fixed-modulus pulse loses its stability against an oscillating-modulus pulse for $\mu_0=-0.20$, which is consistent with the theoretical prediction. In Fig. 6 we show numerical space-time plots for the shape of the pulse in the static and oscillating regimes. Our analytical result is also consistent with numerical observations made in [31], where for the same parameters as before but for $\mu=-0.1$ and varying the dissipation D_r the authors found periodic, quasiperiodic, and chaotic localized solutions. In particular, for $D_r=0.9$ and $\mu=-0.1$, which is greater than our critical value $\mu_0=-0.295$, the authors found a localized solution whose modulus breathes in a periodic fashion with time.

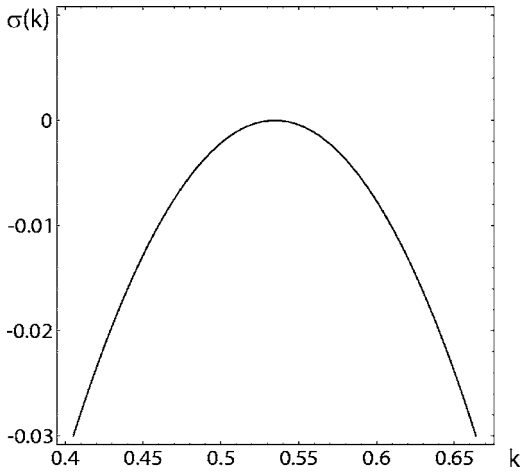

FIG. 5. Values of the parameters are $\beta_r=3.0$, $\beta_i=1.0$, $\gamma_r=-2.75$, $\gamma_i=1.0$, $D_r=0.9$, and $D_i=-1.1$. $\sigma(k)=\mathrm{Re}\,\sigma_k$ vanishes at $k=0.535$ for $\mu=\mu_0=-0.295$. For $\mu<\mu_0$ the function $\sigma(k)$ is negative for all k.

III. THE QUINTIC CGLE WITH NONLINEAR GRADIENT TERMS: MOVING PULSES

As it was mentioned in the Introduction the quintic CGLE including nonlinear gradient terms is a more general model

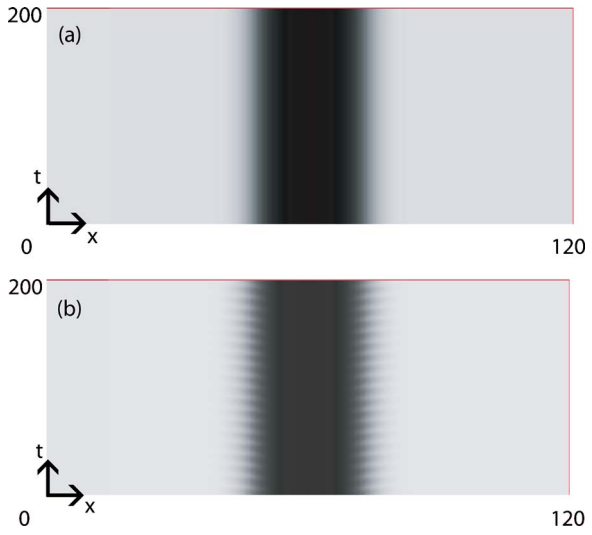

FIG. 6. (Color online) Space-time plots for the modulus of the pulse. Values of the parameters are $\beta_r=3.0$, $\beta_i=1.0$, $\gamma_r=-2.75$, $\gamma_i=1.0$, $D_r=0.9$, and $D_i=-1.1$. (a) For $\mu=-0.21$ the shape of the pulse is static. (b) For $\mu=-0.19$ the shape of the pulse is oscillating.

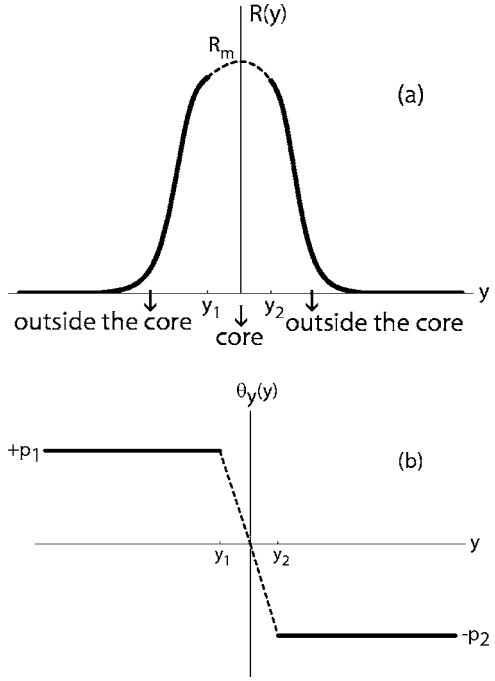

FIG. 7. Analytical approximation for the pulse in the moving frame. For the left ($y<0$) and right sides ($y>0$) the space is divided in two regions: outside the core, where the wave vector is constant, and core, where the wave vector is a straight line. (a) Modulus of the pulse. (b) Wave vector.

with application in propagation of ultrashort pulses in optical fibers [35]:

$$\partial_t A = \mu A + \beta|A|^2 A + \gamma|A|^4 A + D\partial_{xx}A + \lambda\partial_x(|A|^2 A) + \eta A\partial_x(|A|^2). \quad (15)$$

The parameters β, γ, D, λ, and η are, in general, complex. The parameters λ and η break the parity symmetry $x \to -x$ leading to moving pulses.

We stress the fact that the parameters λ and η are not related to the existence of the pulses but are responsible for the velocity and asymmetry of the moving localized structures.

In this section we shall consider μ, γ, and λ real, $\beta=\beta_r+i\beta_i$, $D=1$, and $\eta=0$.

Making the change of variables: $y=x-vt$; $\tau=t$, where v is the velocity of the pulse, we assume that in the moving frame we can do the following Ansatz: $r=R(y)$; $\phi=\Omega\tau+\theta(y)$. Then Eq. (15) reduces to

$$-(v+3\lambda R^2)R_y = \mu R + \beta_r R^3 + \gamma R^5 + R_{yy} - R\theta_y^2, \quad (16)$$

$$-(v+\lambda R^2)R\theta_y = -\Omega R + \beta_i R^3 + 2R_y\theta_y + R\theta_{yy}. \quad (17)$$

As in the previous sections, the strategy to calculate approximately $R(y)$, $\theta_y(y)$, Ω, and v consists in considering that $\theta_y(y)$ (the wave vector) is constant ($+p_1$ for $y<y_1$, $-p_2$ for $y>y_2$) in almost all the domain (outside the core) except in a narrow domain around the center of the pulse (core), where $\theta_y(y)$ is considered to be a straight line [see Fig. 7(b)].

Because of parity breaking the left and right sides of the pulse must be studied separately.

Outside the core and for the left side ($y<y_1$), Eqs. (16) and (17) lead to

$$0 = (\mu^{(1)} - p_1^2)R + \beta^{(1)}R^3 + \gamma^{(1)}R^5 + R_{yy}, \quad (18)$$

where

$$\mu^{(1)} = \mu - \frac{v^2}{2} + \frac{v}{2}\sqrt{v^2+4(p_1^2-\mu)},$$

$$\beta^{(1)} = \beta_r - 2\lambda v - \frac{v\beta_i}{2p_1} + \frac{3}{2}\lambda\sqrt{v^2+4(p_1^2-\mu)},$$

$$\gamma^{(1)} = \gamma - \frac{3}{2}\lambda^2 - \frac{3\lambda\beta_i}{2p_1}. \quad (19)$$

Asymptotically, for $y\to-\infty$ we obtain $\Omega = p_1\sqrt{v^2+4(p_1^2-\mu)}$, which is a constant in $(-\infty,0)$.

For the right side ($y>y_2$) one finds the same equation (18) with coefficients

$$\mu^{(1)} = \mu - \frac{v^2}{2} - \frac{v}{2}\sqrt{v^2+4(p_2^2-\mu)},$$

$$\beta^{(1)} = \beta_r - 2\lambda v + \frac{v\beta_i}{2p_2} - \frac{3}{2}\lambda\sqrt{v^2+4(p_2^2-\mu)},$$

$$\gamma^{(1)} = \gamma - \frac{3}{2}\lambda^2 + \frac{3\lambda\beta_i}{2p_2}. \quad (20)$$

For $y\to+\infty$ we get $\Omega=p_2\sqrt{v^2+4(p_2^2-\mu)}$, which is a constant in $(0,+\infty)$.

Integrating Eq. (18) it is possible to obtain an explicit expression for $R(y)$:

$$R(y) = \frac{2b^{1/4}\exp\{\sqrt{-\mu^{(1)}+p^2}(|y|+y_0)\}}{\sqrt{\left[\exp\{2\sqrt{-\mu^{(1)}+p^2}(|y|+y_0)\}+\frac{a}{\sqrt{b}}\right]^2-4}}, \quad (21)$$

where $a=(-3\beta^{(1)})/2\gamma^{(1)}$, $b=-3(-\mu^{(1)}+p^2)/\gamma^{(1)}$, y_0 is a constant to be determined, $p=p_1$ for $y<y_1$, and $p=-p_2$ for $y>y_2$.

Inside the core and for the left side ($y_1<y<0$) we assume that $R(y)=R_m^{(left)}-\epsilon y^2-\rho y^3$ and $\theta_y=-\alpha y$, where $R_m^{(left)}$ is the highest value of the pulse constructed on the left side. From Eqs. (16) and (17) we can calculate the values of ϵ, ρ, and α:

$$\epsilon = \frac{1}{2}[\mu R_m^{(left)} + \beta_r(R_m^{(left)})^3 + \gamma_r(R_m^{(left)})^5],$$

$$\rho = -\frac{\epsilon}{3}[v+3\lambda(R_m^{(left)})^2],$$

$$\alpha = \beta_i(R_m^{(left)})^2 - \Omega. \quad (22)$$

Imposing continuity of the amplitude $R(y)$, the phase gradient $\theta_y(y)$, and the derivative of the amplitude of the analytical expressions calculated inside and outside the core of the pulse at $y=y_1=-p_1/\alpha$ we determine y_0 and a relation between $R_m^{(left)}$ and p_1:

$$f_1(R_m^{(left)},p_1) \equiv \sqrt{-\frac{\gamma^{(1)}}{3}} r_c \sqrt{r_c^4 - a r_c^2 + b} + 2\epsilon y_1 + 3\rho y_1^2 = 0, \tag{23}$$

where $r_c = R_m^{(left)} - \epsilon y_1^2 - \rho y_1^3$.

In order to obtain a second relation between $R_m^{(left)}$ and p_1 we use a *consistency relation* by multiplying Eq. (17) by $R(y)$ and integrating from $-\infty$ to 0.

$$g_1(R_m^{(left)},p_1) \equiv \Omega - \frac{1}{(I_2^{(0)} + I_2^{(1)})}\{\beta_i(I_4^{(0)} + I_4^{(1)}) + v(p_1 I_2^{(0)} + I_2^{(2)}) + \lambda(p_1 I_4^{(0)} + I_4^{(2)})\} = 0, \tag{24}$$

where $I_2^{(0)} \equiv \int_{-\infty}^{y_1} R^2\, dy$, $I_4^{(0)} \equiv \int_{-\infty}^{y_1} R^4\, dy$, $I_2^{(1)} \equiv \int_{y_1}^{0} R^2\, dy$, $I_4^{(1)} \equiv \int_{y_1}^{0} R^4\, dy$, $I_2^{(2)} \equiv \int_{y_1}^{0} R^2 \theta_y\, dy$, and $I_4^{(2)} \equiv \int_{y_1}^{0} R^4 \theta_y\, dy$, which can be calculated explicitly.

For the right side ($y>0$) we proceed in an analogous way obtaining a relation between $R_m^{(right)}$ and p_2:

$$f_2(R_m^{(right)},p_2) \equiv \sqrt{-\frac{\gamma^{(1)}}{3}} r_c \sqrt{r_c^4 - a r_c^2 + b} - 2\epsilon y_2 - 3\rho y_2^2 = 0, \tag{25}$$

where $r_c = R_m^{(right)} - \epsilon y_2^2 - \rho y_2^3$, and a *consistency relation* given by

$$g_2(R_m^{(right)},p_2) \equiv \Omega - \frac{1}{(I_2^{(0)} + I_2^{(1)})}\{\beta_i(I_4^{(0)} + I_4^{(1)}) - v(p_2 I_2^{(0)} - I_2^{(2)}) - \lambda(p_2 I_4^{(0)} - I_4^{(2)})\} = 0, \tag{26}$$

where $I_2^{(0)} \equiv \int_{y_2}^{+\infty} R^2\, dy$, $I_4^{(0)} \equiv \int_{y_2}^{+\infty} R^4\, dy$, $I_2^{(1)} \equiv \int_{0}^{y_2} R^2\, dy$, $I_4^{(1)} \equiv \int_{0}^{y_2} R^4\, dy$, $I_2^{(2)} \equiv \int_{0}^{y_2} R^2 \theta_y\, dy$, and $I_4^{(2)} \equiv \int_{0}^{y_2} R^4 \theta_y\, dy$, which can be calculated explicitly.

Thus for fixed values of Eq. (15) and v, expressions (23)–(26) give us $R_m^{(left)}$, $R_m^{(right)}$, p_1, and p_2, which enable us to determine the left and right parts of the localized structure. Finally, the continuity of the pulse at $y=0$ or the condition

$$R_m^{(left)}(v) = R_m^{(right)}(v) \tag{27}$$

leads to two values of v (velocity of the pulse), namely, $v=v_u$, the velocity of the unstable pulse, and $v=v_s$, the velocity of the stable pulse.

To verify this analytical prediction in a concrete case we fix the parameters of Eq. (15): $\mu=-0.5$, $\beta_r=3.0$, $\beta_i=1.0$, $\gamma=-2.75$, and $\lambda=-0.1$.

Figures 8(a) and 8(b) show that for $v=v_u=0.056\,75$ relation (27) is satisfied and $R_m^{(left)}(v_u)=R_m^{(rright)}(v_u)=0.647\,96$. In addition $p_1=0.189\,99$ and $p_2=0.187\,52$. Thus the unstable pulse is completely determined.

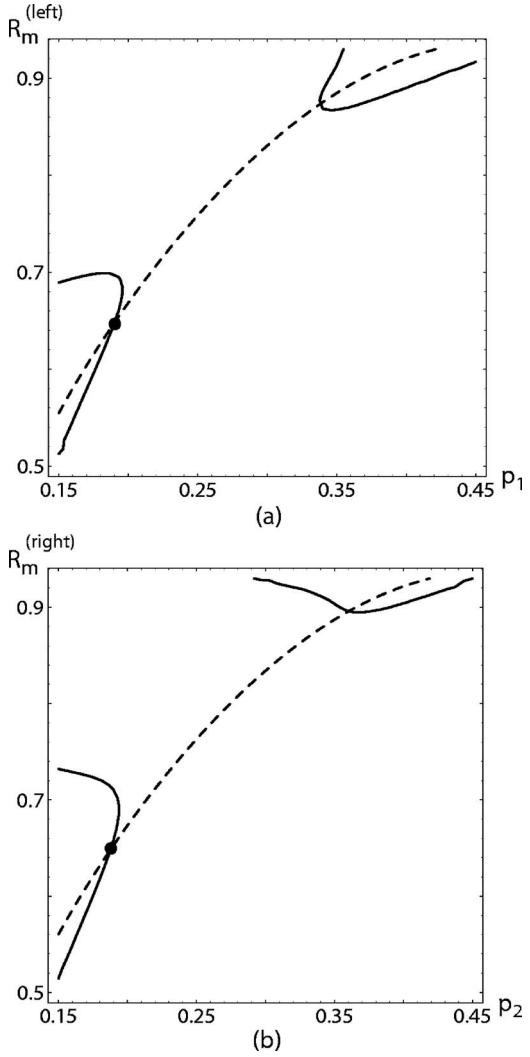

FIG. 8. Parameters of Eq. (15) are $\mu=-0.5$, $\beta_r=3.0$, $\beta_i=1.0$, $\gamma=-2.75$, and $\lambda=-0.1$. (a) The intersection (solid circle) between the curves $f_1(R_m^{(left)},p_1)=0$ (continuous line) and $g_1(R_m^{(left)},p_1)=0$ (dashed line) predicts the left side of the unstable pulse. (b) The intersection (solid circle) between the curves $f_2(R_m^{(right)},p_2)=0$ (continuous line) and $g_2(R_m^{(right)},p_2)=0$ (dashed line) predicts the right side of the unstable pulse. For $v=v_u=0.05675$ relation $R_m^{(left)}(v_u)=R_m^{(right)}(v_u)=0.64796$ is satisfied. In addition $p_1=0.189\,99$ and $p_2=0.187\,52$.

Figures 9(a) and 9(b) show that for $v=v_s=0.090\,61$ relation (27) is satisfied and $R_m^{(left)}(v_s)=R_m^{(right)}(v_s)=0.885\,26$. In addition $p_1=0.351\,86$ and $p_2=0.345\,81$. Thus the stable pulse is completely determined.

Moreover we can study the relation between v_s and λ. We find analytically and from direct numerical simulations that v_s varies linearly with λ. For $|\lambda|>0.1$ our method collapses for the parameters used in this example. The reason may be the fact that for large v the renormalized parameters $\mu^{(1)}$, $\beta^{(1)}$, and $\gamma^{(1)}$ lead to a pulse outside the analytical stability tongue. This is an indication that for large $|\lambda|$ the pulse expands (transition to fronts). We have observed this behavior numerically.

In Fig. 10(a) we show the shapes of the pulses obtained with the analytical approach. The continuous line represents

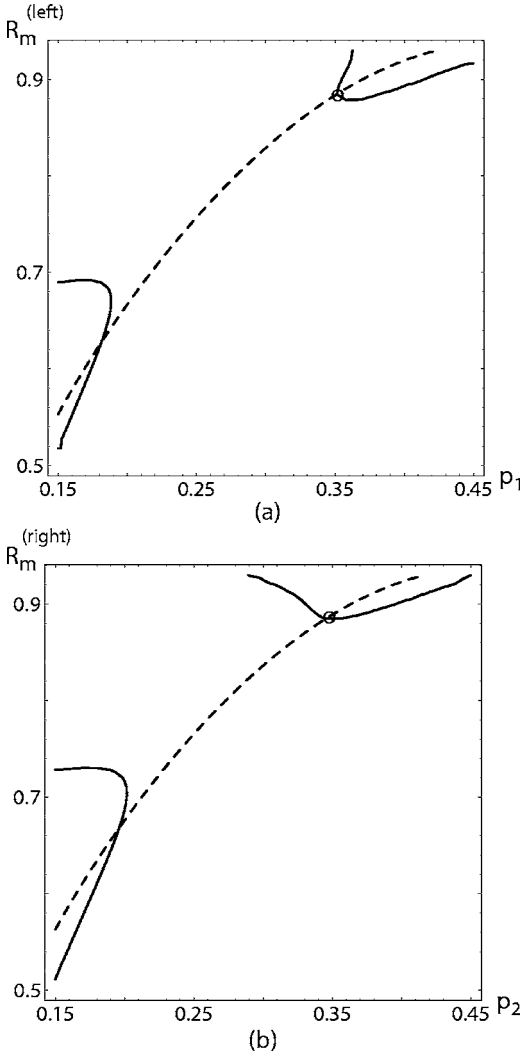

FIG. 9. Parameters of Eq. (15) are $\mu=-0.5$, $\beta_r=3.0$, $\beta_i=1.0$, $\gamma=-2.75$, and $\lambda=-0.1$. (a) The intersection (open circle) between the curves $f_1(R_m^{(left)},p_1)=0$ (continuous line) and $g_1(R_m^{(left)},p_1)=0$ (dashed line) predicts the left side of the stable pulse. (b) The intersection (open circle) between the curves $f_2(R_m^{(right)},p_2)=0$ (continuous line) and $g_2(R_m^{(right)},p_2)=0$ (dashed line) predicts the right side of the stable pulse. For $v=v_s=0.090\,61$ relation $R_m^{(left)}(v_s)=R_m^{(right)}(v_s)=0.885\,26$ is satisfied. In addition $p_1=0.351\,86$ and $p_2=0.345\,81$.

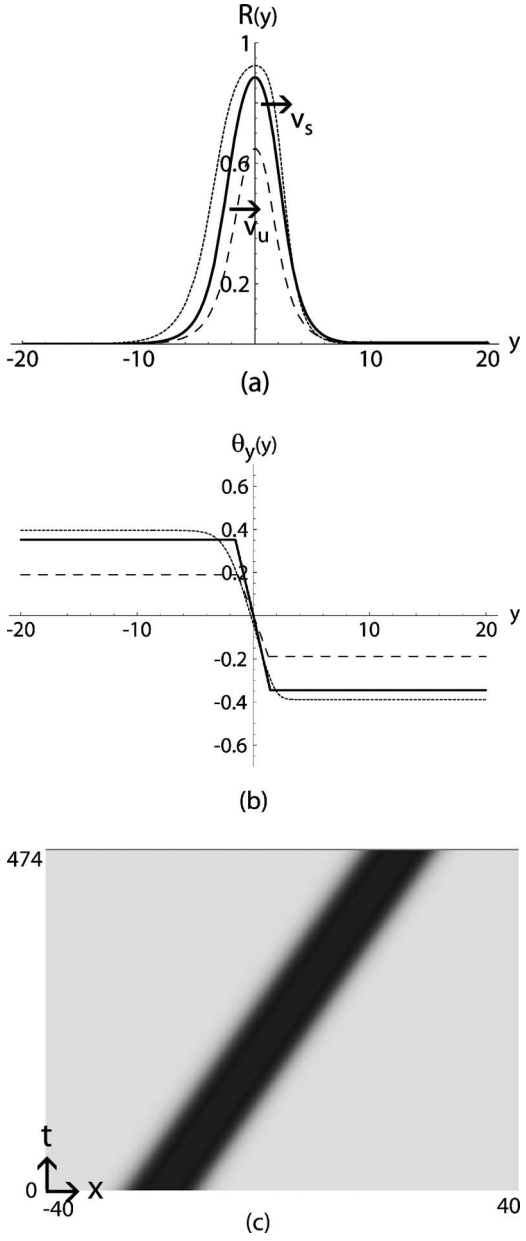

FIG. 10. Parameters of Eq. (15) are $\mu=-0.5$, $\beta_r=3.0$, $\beta_i=1.0$, $\gamma=-2.75$, and $\lambda=-0.1$. (a) Shape of the stable and unstable pulses predicted by the analytical approach (continuous and dashed lines). The numerical result for the stable pulse is represented by punctured line. v_s and v_u are the velocities of the stable and unstable pulses, respectively. (b) The wave vector. (c) Numerical space-time plot for the shape of the stable moving pulse.

the stable pulse and the dashed line the unstable one. The stable pulse obtained from a direct numerical simulation is drawn with a punctured line. In Fig. 10(b) we show the wave vector for the three above-mentioned cases. Figure 10(c) shows a numerical space-time plot for the modulus of the stable moving pulse, which leads to a numerical velocity of the pulse $v=0.084\,21$. The analytical values of R_m, v, and the asymptotical values of the wave vector for the stable moving pulse agree with direct numerical simulations within 4%, 8%, and 10% respectively.

IV. HOLES IN THE QUINTIC CGLE

Another large class of localized solutions are hole solutions. They have already been shown to exist for the cubic CGLE [37,38], but are known to be unstable against small changes in the equations (structural instability) [39].

The quintic CGLE (1) admits stable stationary hole solutions with most parameters being real [40]. In this section we consider μ, γ, and D real, $\beta=\beta_r+i\beta_i$.

Carrying out the following Ansatz: $r=R(x)$; $\phi=\Omega t+\theta(x)$, Eq. (1) reduces to

$$0=\mu R+\beta_r R^3+\gamma R^5+D(R_{xx}-R\theta_x^2), \tag{28}$$

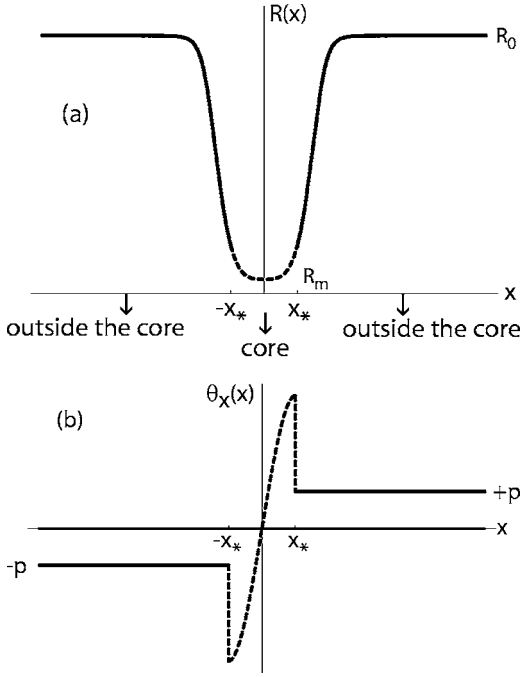

FIG. 11. Analytical approximation for the stationary hole. The space is divided in two regions: outside the core, where the wave vector is constant, and core, where the wave vector is a cubic function. The value $x=x_*$ corresponds to the local maximum of the cubic function. (a) Modulus of the pulse. (b) Wave vector.

$$R\Omega = \beta_i R^3 + D(R\theta_{xx} + 2R_x\theta_x). \tag{29}$$

The strategy to approximately calculate $R(x)$, $\theta(x)$, and Ω consists in considering that $\theta_x(x)$ (the wave vector) is constant ($-p$ for the left side, $+p$ for the right side) in almost all the domain (outside the core) except in a narrow domain around the center of the hole (core), where $\theta_x(x)$ is considered to be a cubic function (see Fig. 11).

Outside the core ($|x|>x_*$), Eqs. (28) and (29) lead to

$$0 = (\mu - Dp^2)R + \beta_r R^3 + \gamma R^5 + DR_{xx}, \tag{30}$$

$$R\Omega = \beta_i R^3 \pm 2DpR_x. \tag{31}$$

Asymptotically, for $x\to\infty$, from the above equations we obtain R_0, the asymptotic value of the modulus of the stationary hole, and its frequency Ω:

$$R_0 = \sqrt{\frac{-\beta_r - \sqrt{\beta_r^2 - 4\gamma(\mu - Dp^2)}}{2\gamma}},$$

$$\Omega = -\frac{\beta_i}{2\gamma}[\beta_r + \sqrt{\beta_r^2 - 4\gamma(\mu - Dp^2)}].$$

By integrating Eq. (31) it is possible to obtain an explicit expression for $R(x)$:

$$R(x) = \frac{R_0}{\sqrt{1 + \exp\left\{-\frac{\Omega}{Dp}(|x| - x_0)\right\}}}, \tag{32}$$

where x_0 is a constant to be determined, which is related to the translational symmetry of Eq. (31).

Inside the core ($|x|<x_*$) we assume that $R(x)=R_m+\epsilon x^2+\delta x^4$ and $\theta_x=\alpha x-\beta x^3$, where R_m is the height of the hole at $x=0$. Then $x_*=\sqrt{\alpha/3\beta}$.

From Eqs. (28) and (29) we can calculate the values of ϵ, δ, α, and β in terms of R_m, Ω, and the parameters of Eq. (1).

Imposing continuity of the amplitude $R(x)$ at $x=x_*$ we obtain $x_0=x_*+Dp/\Omega\,\ln|R_0^2/r_c^2-1|$, where $r_c=R(x_*)$. The continuity of the first derivative of the amplitude $R(x)$ leads to a first relation between R_m and p:

$$f(p,R_m) \equiv \frac{r_c\Omega(R_0^2 - r_c^2)}{2Dp\,R_0^2} - 2\epsilon x_* - 4\delta x_*^3 = 0. \tag{33}$$

In order to obtain a second relation between R_m and p we use a consistency relation by multiplying Eq. (29) by $R(x)$ and integrating from 0 to ∞. Taking into account that expression (32) represents an exact solution of Eq. (29) the above consistency relation reduces to

$$g(p,R_m) \equiv \Omega\int_0^{x_*} R^2\,dx - \beta_i\int_0^{x_*} R^4\,dx - Dp\,r_c^2 = 0. \tag{34}$$

Thus we have constructed approximate expressions for $R(x)$ and $\theta_x(x)$ in all the domain in terms of two unknown parameters, namely, R_m and p. The existence of stationary holes is related to the intersection between the curves $f(p,R_m)=0$ and $g(p,R_m)=0$.

For Eq. (1), and for fixed parameters μ, β_r, γ, and D we found the following scenario: there exists a critical value β_{ic1} so that for $\beta_i<\beta_{ic1}$ the curves $f(p,R_m)=0$ and $g(p,R_m)=0$ do not intersect at any point suggesting there are no holes. For $\beta_i>\beta_{ic1}$ the curves intersect in two points leading to a stable and an unstable hole via a saddle-node bifurcation. By further increasing β_i we find another critical value β_{ic2} so that for $\beta_i>\beta_{ic2}$ there still exist an intersection between the curves $f=g=0$ predicting an unstable hole, but the stable hole disappears.

For fixed parameters of Eq. (1): $\mu=-0.06$; $\beta_r=1.125$; $\gamma_r=-0.859375$; and $D=1$, the above analytical scenario predicts stable holes in the range $\beta_i\in[0.43,0.50]$. A numerical simulation of Eq. (1) with periodic boundary conditions leads to stable stationary holes in the range $\beta_i\in[0.456,0.503]$, which is in good agreement with our theoretical prediction.

V. CONCLUSIONS AND PERSPECTIVE

In this paper we have studied analytically the appearance of static and oscillating modulus in the quintic CGLE without nonlinear gradient terms, and moving pulses in the quintic CGLE including nonlinear gradient terms. We focused on this equation since it represents a prototype envelope equation associated with the onset of an oscillatory instability

near a weakly inverted bifurcation. The used analytical method, valid through the whole intermediate range of parameters between the variational and conservative limits, consists of calculating the localized structure inside and outside the core and then to match the approximate solutions in the border of the regions, imposing there continuity of the amplitude, the phase, and the derivative of the amplitude. The principal results concerning the quintic CGLE without nonlinear gradients are the appearance of pulses with fixed shape is related to a saddle-node bifurcation, and a linear analysis gives an indication for the existence of pulses with oscillating modulus. For the quintic CGLE including nonlinear gradient terms, the method enables us to calculate the velocities of the stable and unstable moving pulses. In all cases the results obtained using the analytic approximation scheme are in good agreement with direct numerical simulations. Finally, we have briefly showed the usefulness of this method in predicting the range of existence of other classes of localized solutions in the quintic CGLE, namely, stable holes. We conjecture that this successful method for the quintic CGLE could be useful in studying systematically localized structures resulting from other mechanisms different from the coexistence between a limit cycle and a fixed point.

ACKNOWLEDGMENTS

O.D. wishes to acknowledge the support of FAI (Project No. ICIV-001-04, Universidad de los Andes), FONDECYT (Project Nos. 1050660 and 1020374), and Project No. ACT15 (Anillo en Ciencia y Tecnología). The author are grateful to Dr. Pablo Zegers for a critical reading of this manuscript.

[1] P. Kolodner, D. Bensimon, and C. M. Surko, Phys. Rev. Lett. **60**, 1723 (1988).
[2] Y. A. Astrov and Y. A. Logvin, Phys. Rev. Lett. **79**, 2983 (1997).
[3] B. Schäpers, M. Feldmann, T. Ackemann, and W. Lange, Phys. Rev. Lett. **85**, 748 (2000).
[4] P. Umbanhowar, F. Melo, and H. L. Swinney, Nature (London) **382**, 793 (1996).
[5] H. H. Rotermund, S. Jakubith, A. von Oertzen, and G. Ertl, Phys. Rev. Lett. **66**, 3083 (1991).
[6] K. J. Lee, W. D. McCormick, Q. Ouyang, and H. L. Swinney, Nature (London) **369**, 215 (1994).
[7] P. Coullet, C. Riera, and C. Tresser, Phys. Rev. Lett. **84**, 3069 (2000).
[8] J. E. Pearson, Science **261**, 189 (1993).
[9] Y. Hayase and T. Ohta, Phys. Rev. Lett. **81**, 1726 (1998).
[10] K. Krischer and A. Mikhailov, Phys. Rev. Lett. **73**, 3165 (1994).
[11] C. P. Schenk, M. Or-Guil, M. Bode, and H.-G. Purwins, Phys. Rev. Lett. **78**, 3781 (1997).
[12] J. Kosek and M. Marek, Phys. Rev. Lett. **74**, 2134 (1995).
[13] S. Koga and Y. Kuramoto, Prog. Theor. Phys. **63**, 106 (1980).
[14] T. Ohta, Y. Hayase, and R. Kobayashi, Phys. Rev. E **54**, 6074 (1996).
[15] Y. Hayase, O. Descalzi, and H. R. Brand, Phys. Rev. E **69**, 065201(R) (2004).
[16] M. C. Cross and P. C. Hohenberg, Rev. Mod. Phys. **65**, 851 (1993).
[17] H. Sakaguchi and H. R. Brand, Physica D **117**, 95 (1998).
[18] O. Thual and S. Fauve, J. Phys. (France) **49**, 1829 (1988).
[19] B. A. Malomed, Physica D **29**, 155 (1987).
[20] S. Fauve and O. Thual, Phys. Rev. Lett. **64**, 282 (1990).
[21] V. Hakim and Y. Pomeau, Eur. J. Mech. B/Fluids **10**, 137 (1991).
[22] B. A. Malomed and A. A. Nepomnyashchy, Phys. Rev. A **42**, 6009 (1990).
[23] W. van Saarloos and P. C. Hohenberg, Phys. Rev. Lett. **64**, 749 (1990).
[24] W. van Saarloos and P. C. Hohenberg, Physica D **56**, 303 (1992).
[25] P. Marcq, H. Chaté, and R. Conte, Physica D **73**, 3035 (1994).
[26] N. Akhmediev and V. V. Afanasjev, Phys. Rev. Lett. **75**, 2320 (1995).
[27] N. N. Akhmediev, V. V. Afanasjev, and J. M. Soto-Crespo, Phys. Rev. E **53**, 1190 (1996).
[28] V. V. Afanasjev, N. Akhmediev, and J. M. Soto-Crespo, Phys. Rev. E **53**, 1931 (1996).
[29] J. M. Soto-Crespo, N. N. Akhmediev, V. V. Afanasjev, and S. Wabnitz, Phys. Rev. E **55**, 4783 (1997).
[30] N. Akhmediev, J. M. Soto-Crespo, and G. Town, Phys. Rev. E **63**, 056602 (2001).
[31] R. J. Deissler and H. R. Brand, Phys. Rev. Lett. **72**, 478 (1994).
[32] R. J. Deissler and H. R. Brand, Phys. Rev. Lett. **81**, 3856 (1998).
[33] O. Descalzi, M. Argentina, and E. Tirapegui, Phys. Rev. E **67**, 015601(R) (2003).
[34] O. Descalzi, Y. Hayase, and H. R. Brand, Phys. Rev. E **69**, 026121 (2004).
[35] H. Tian, Z. Li, J. Tian, and G. Zhou, Phys. Rev. E **66**, 066204 (2002).
[36] E. J. Doedel, H. B. Keller, and J. P. Kernévez, Eur. J. Biochem. **1**(4), 745 (1991).
[37] K. Nozaki and N. Bekki, J. Phys. Soc. Jpn. **53**, 1581 (1984).
[38] H. Sakaguchi, Prog. Theor. Phys. **85**, 417 (1991).
[39] I. Aranson and L. Kramer, Rev. Mod. Phys. **74**, 99 (2002).
[40] H. Sakaguchi, Prog. Theor. Phys. **86**, 7 (1991).